

NUMERICAL ANALYSIS OF TEMPERATURE FIELD DURING HARDFACING PROCESS AND COMPARISON WITH EXPERIMENTAL RESULTS

by

**Vukic N. LAZIĆ¹, Ivana B. IVANOVIĆ², Aleksandar S. SEDMAK³,
Rebeka RUDOLF⁴, Mirjana M. LAZIĆ⁵ and Zoran J. RADAKOVIĆ³**

¹Faculty of Mechanical Engineering, University of Kragujevac, Serbia

²Innovation Center of Faculty of Mechanical Engineering, University of Belgrade, Belgrade, Serbia

³Faculty of Mechanical Engineering, University of Belgrade, Serbia

⁴ Faculty of Mechanical Engineering, University of Maribor, Maribor, Slovenia

⁵Faculty of Sciences, University of Kragujevac, Kragujevac, Serbia

Original scientific paper

DOI: 10.2298/TSC1130117177L

The three-dimensional transient nonlinear thermal analysis of the hard facing process is performed by using the finite element method. The simulations were executed on the open source Salome platform using the open source finite element solver Code Aster. The Gaussian double ellipsoid was selected in order to enable greater possibilities for the calculation of the moving heat source. The numerical results were compared with available experimental results.

Keywords: *welding simulations; transient heat conduction; moving heat source;*

Introduction

In the case of numerical analysis of the temperature field, the hard facing process belongs to a group of welding problems which are usually simulated as three-dimensional transient heat transfer problems, and also nonlinear if the thermal properties of the material are treated as temperature dependent. The most important issue of numerical model is the moving heat source.

The way in which the process is simulated numerically is a great simplification of the real process. The model is most often a plate with the heat source moving along one axis with constant velocity. Calculations are straightforward but, due to the size of the plate for example, they can be demanding in computation time and memory, and still do not give completely reliable results. For a long time numerous experimental and numerical studies have been dealing with different aspects of the problem, [1-5]. There is a wide range of functions for the heat source implementation, but the most accepted is certainly the double ellipsoidal heat source, [6]. Recently, those studies dealing with a reliability of both, experimental and numerical results have become significant, [7-11].

The model for this numerical analysis was a plate that was chosen from a very extensive experimental analysis of the hard facing process given in [12]. During selection priority was given to a group of measurements that provide most information for the setup of

*Corresponding author, e-mail: vlazic1@sbb.rs

the numerical model and for the validation of numerical results. The initial idea was to ensure accurate numerical results of the temperature field that would be used for the future mechanical analysis of the same model.

Model description

The models are two plates selected from a series of setups used for experimental analysis in [12]. The plates are made of unalloyed medium carbon steel, JUS Č1530 (DIN C45), they have different thicknesses, 20 mm and 21 mm, while the lengths and widths are the same, 430 mm, and 200 mm respectively.

As in experimental analysis from [12], numerical simulations were performed for two different heat sources with the characteristics listed in Table 1.

Table 1. Characteristics of heat sources used for experimental measurements

Electrode diameter [mm]	Arc voltage [V]	Arc current [A]	Welding velocities [cm/s]	Heat input [J/cm]
4	25.6	140	0.162 – 0.136	17650 – 21101
5	28.5	210	0.286 – 0.098	16736 – 48610

The experimental results for the point in the symmetry plane, at 4 mm below the top surface, for five cases that were selected for numerical analysis, are presented in Table 2.

Table 2. Experimental results for JUS Č1530 (DIN C45) steel

Case number	Plate thickness [mm]	Electrode diameter [mm]	Heat input [J/cm]	Initial temperature [°C]	Cooling time from 800 to 500°C [s]
1	20	4	17975	50	7.5
2			19809	20	8.5
3			21101	20	9.5
4	21	5	35817	100	28
5			35692	20	16

The maximal values of temperature in the heat affected zone, measured at a point located 4 mm below the top surface of the plate in the symmetry plane, are given for the first case and the fourth case, $T_{\max} = 1145^{\circ}\text{C}$, and $T_{\max} = 959^{\circ}\text{C}$ respectively. These two cases were used for the calibration of the numerical heat source.

Numerical solution

The geometry of the model used in numerical simulations is a well-known half plate model. This model is usually chosen since the temperature field can be treated symmetrically with respect to the path of the heat source moving along one axis with constant velocity. Here, the heat source was moving with a constant velocity along the x axis, the top half-surface was placed in the x-y plane, and the symmetry plane coincides with the x-z plane.

A temperature dependent thermal conductivity and volumetric heat capacity of JUS Č1530 (DIN C45) steel, illustrated in Figure 1, were included in the calculations.

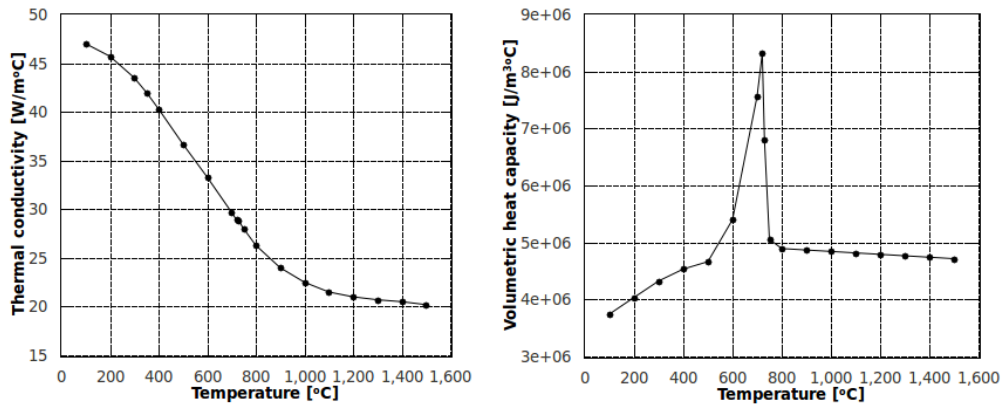


Figure 1. Thermal properties of the JUS C1530 (DIN C45) steel as function of temperature

Calculations were performed on the open source Salome platform using the open source finite element solver Code Aster, [13]. The thermal problem has been simulated as three-dimensional transient and also nonlinear as thermal properties are temperature dependent. Besides the symmetry plane where the zero flux condition was imposed at the boundary, at all other surfaces convection boundary conditions were imposed outside the influence of the heat source. For the volumetric heat source the Gaussian double ellipsoid was used, [6].

When the heat source is moving along the x-axis the double ellipsoid is given by the following equation

$$q(x, y, z, t) = \frac{6\sqrt{3} \cdot fQ}{abc\pi \cdot \sqrt{\pi}} \cdot e^{-3[x-(x_0+v_s t)]^2/a^2} \cdot e^{-3y^2/b^2} \cdot e^{-3z^2/c^2}$$

where Q is the power, v_s is the velocity, and x_0 is the initial position of the heat source. Parameters a , b , and c are the semi-axis of the ellipsoid. Since it is a double ellipsoid, the front and rear values of parameter a are different, a_f and a_r , as well as front and rear values of parameter f

$$f_f = \frac{2a_f}{a_f + a_r} \text{ and } f_r = 2 - f_f$$

The same mesh of 134160 hexahedral elements was used in all simulations. The number of segments 1D hypothesis with equidistant distribution was used in x direction (215 segments). The same 1D hypothesis was used for the first 5 mm in they and z direction (5 segments), and for the rest the arithmetic 1D hypothesis was applied with a start length of 1 mm and an end length of 3 mm.

Results and discussion

For all simulations, the time step was set to 1 s, the heat transfer coefficient to 10 W/m²°C, the initial position of the heat source to 6 mm, the heat source efficiency to 0.8, and the ambient temperature was set to be equal to the initial temperature of the plate. Since calculations were executed on a desktop PC with Intel Core i5-2300 CPU on 2.8 GHz and 16GB RAM memory, with the same mesh distribution, and with the same time step value, one time step lasted for approximately 2 minutes of CPU time.

The first series of simulations was performed for the case 1 in Table 2. For the heat input given in Table 2, characteristics of the heat source given in Table 1, and the efficiency of 0.8, the velocity of the heat source is 1.5951 mm/s which was rounded to $v_s = 0.0016$ m/s in calculations. The parameters of the double ellipsoidal heat source have been chosen randomly in order to carry out some kind of calibration of the heat source. The end time of simulations, $t = 50$ s, was chosen so that the temperature at the point (0.05, 0, 0.004) m drops below 500°C. The results are presented in Figure 2.

The three resulting curves in Figure 2 are marked additionally with symbols to highlight the differences. First is the one marked with stars where the semi-axis c of a double ellipsoid is 10 mm. The resulting maximal temperature is 3418°C and is much higher than the measured temperature of 1145°C. The last two curves have $c = 3$ mm, and other parameters have the same value, which is somewhat higher than in the other calculations, 8 and 10 mm. The resulting maximal temperature is still much higher but is approaching measured maximal temperature.

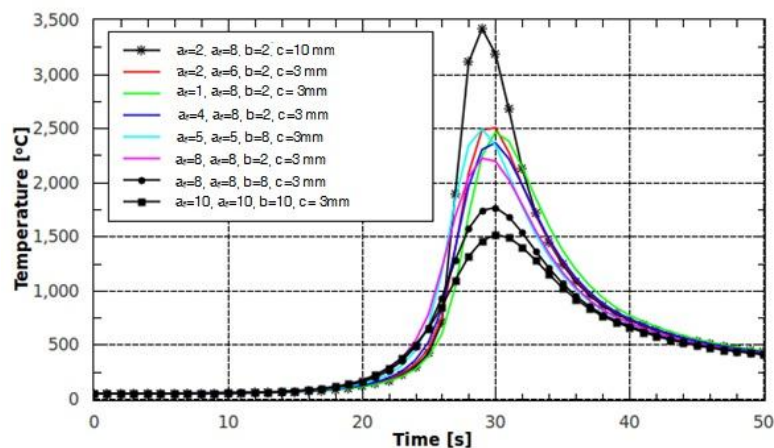


Figure 2. Numerical results for the temperature as a function of time for the first series of randomly selected double ellipsoid parameters for the point in the symmetry plane ($y = 0$), at $x = 0.05$ m and $z = 0.004$ m, obtained for the case 1 in Table 2

The calibration of the heat source has been continued for a couple more combinations of parameters. The results are illustrated in Figure 3. Again, the two resulting curves are marked additionally with symbols to highlight that the maximal temperature reached at the position (0.05, 0, 0.004) m is slightly lower (blue line), or higher (red line), than the measured temperature. The combination of parameters presented with the blue line that results with the maximal temperature of 1110°C was chosen for further calculations that include cases 1-3 from Table 2. At the position $x = 0.05$ m, the constant maximal value of the temperature that will be reached on the plate has still not been reached, which is the reason why the combination of parameters that produces the lower value of maximal temperature is selected for further simulations.

The results obtained for the case 1, with the combination of parameters selected above, for time $t = 125$ s, when the center of the heat source is at the position 0.206 m, is illustrated in Figure 4. The point with experimentally measured results is marked with a blue dot. Since the x position is 0.2 m the constant maximal temperature has been reached. The

maximal temperature at the plate is approximately 2153°C, and the maximal temperature at the selected point is approximately 1136°C (measured temperature is 1145°C).

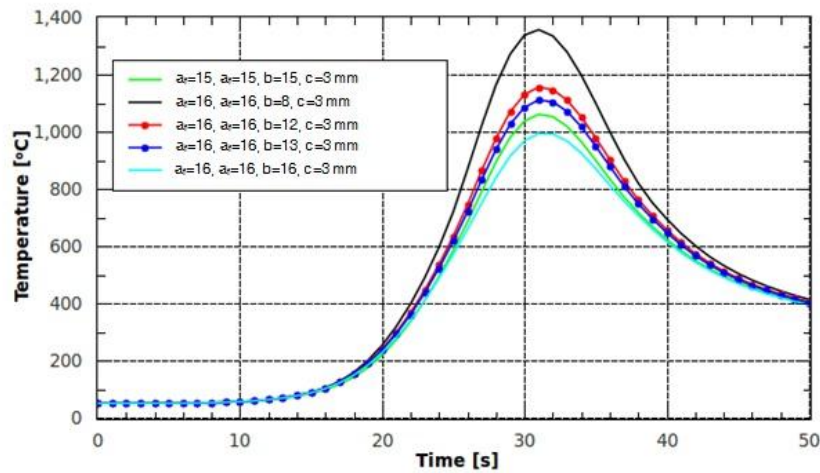


Figure 3. Numerical results for the temperature as a function of time for the second series of randomly selected double ellipsoid parameters for the point in the symmetry plane ($y = 0$), at $x = 0.05$ m and $z = 0.004$ m, obtained for the case 1 in Table 2

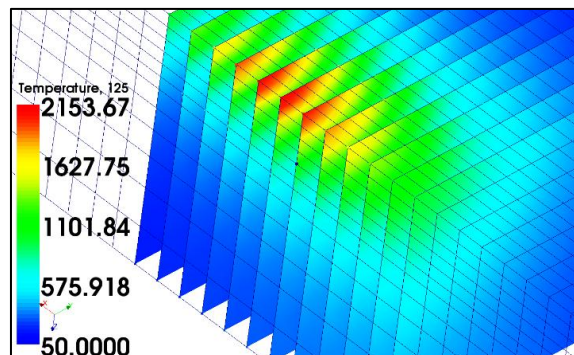


Figure 4. Temperature distribution presented in cut planes distributed at every 2 mm in front and behind the position $x = 0.2$ m at time $t = 125$ s when the temperature reaches the maximal value at the symmetry plane ($y = 0$), at the point $x = 0.2$ m and $z = 0.004$ m (marked with a blue dot).

Simulations were continued for cases 2 and 3. For these cases, the initial temperature of the plate was 20°C, and velocities of the heat source were rounded to $v_s = 0.00145$ m/s, and $v_s = 0.00136$ m/s respectively. The results are illustrated in Figure 5. Values for the cooling time obtained numerically, 7.9 s for case 1, 8.2 s for case 2, and 8.9 s for case 3, are pretty close to the experimentally measured values, 7.5 s for case 1, 8.5 s for case 2, and 9.5 s for case 3.

The calibration of the heat source was repeated for the last two cases from Table 2 and the second heat source from Table 1. The case 4 was used for calibration since the maximal temperature at the point $z = 0.004$ m was measured in the experiment and given in [12]. The value of the velocity of the heat source was rounded to $v_s = 0.00134$ m/s. Results

are presented in Figure 6. The last combination of parameters resulted with the maximal temperature of approximately 933°C which is lower than, and closest to, the measured maximal temperature of 959°C.

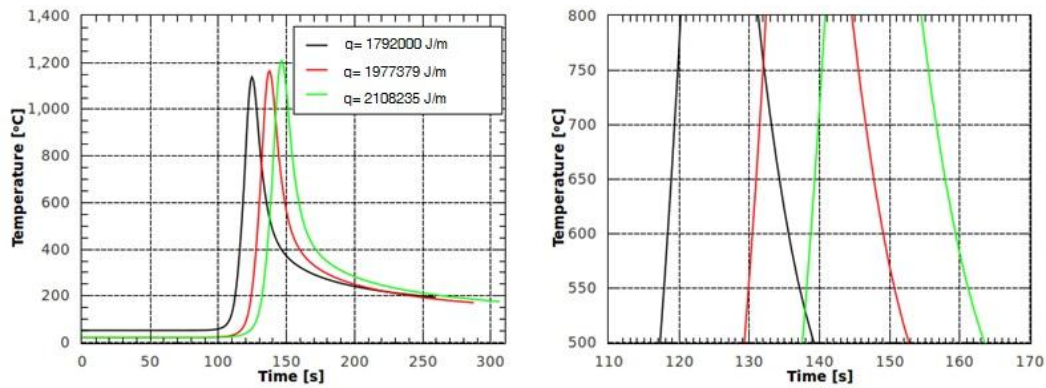


Figure 5. Temperature as a function of time at the position (0.2, 0, 0.004) m for cases 1, 2, and 3 presented in Table 2 (left figure), and cooling time for the same cases (right figure)

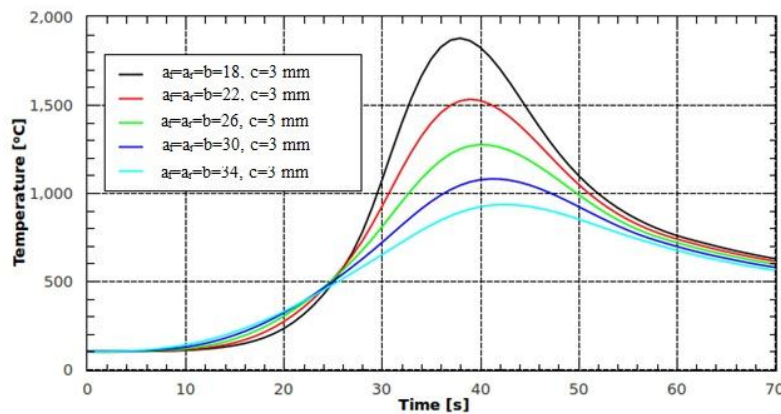


Figure 6. Numerical results for the temperature as a function of time for the series of randomly selected double ellipsoid parameters for the point in the symmetry plane ($y = 0$), at $x = 0.05$ m and $z = 0.004$ m, obtained for the case 4 in Table 2

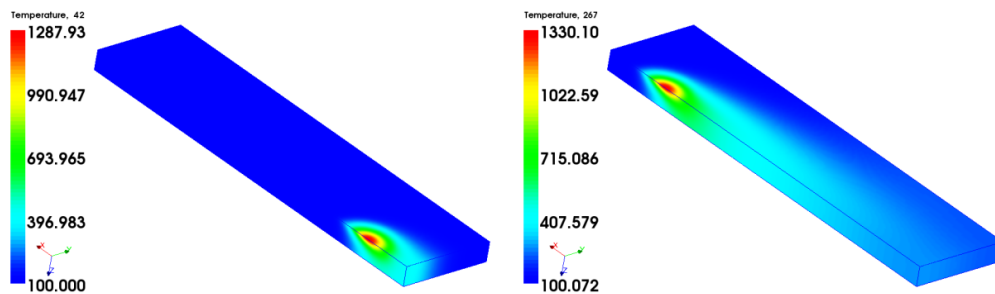


Figure 7. Temperature distribution for the case 4 from Table 2 at $t = 42$ s (left) and $t = 267$ s (right)

The temperature distribution for the last combination of the heat source parameters applied to the fourth case is illustrated in Figure 7. Temperature distribution for this case was chosen to be presented as the most illustrative. The initial temperature of the plate was the highest, the value of the heat input was higher and the velocity was lower than in the previous cases, and therefore the cooling of the plate was slower.

At $t=42$ s, (Figure 7 left), the maximal value of temperature at point $(0.05, 0, 0.004)$ m is reached. At that time, the center of the source is more than 12 mm in front of the point. At $t=267$ s, (Figure 7 right), the maximal value of temperature at point $(0.35, 0, 0.004)$ m is reached and the center of the source is almost 14 mm in front of the point. The maximal temperature of the plate at $t=42$ s is approximately 1288°C while the maximal temperature that was reached on the plate is approximately 1330°C (Figure 7 right).

The temperature distribution in cut planes around the position $x=0.35$ m is illustrated in Figure 8. The maximal temperature at point $(0.35, 0, 0.004)$ m is approximately 982°C . The temperature is 23°C higher than the measured temperature.

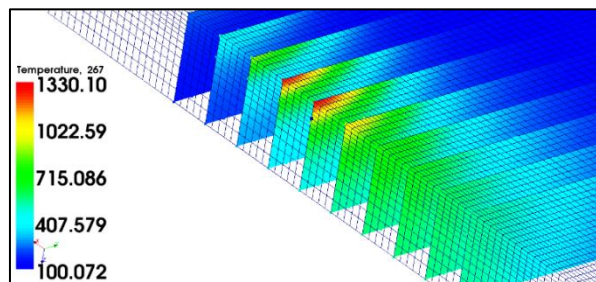


Figure 8. Temperature distribution presented in cut planes distributed at every 10 mm in front and behind the position $x = 0.35$ m at time $t = 267$ s when the temperature reaches the maximal value at the symmetry plane ($y = 0$), at the point $x = 0.35$ m and $z = 0.004$ m (marked with a blue dot).

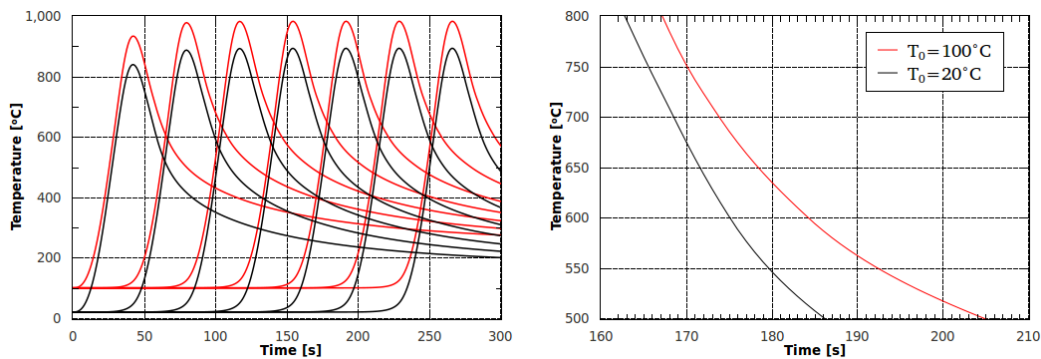


Figure 9. Temperature as a function of time at positions $x = 0.05, 0.1, 0.15, 0.2, 0.25, 0.3, \text{ and } 0.35$ m ($y = 0, z = 0.004$ m) for cases 4-5 presented in Table 2 (left), and cooling time for the same cases (right)

The simulations were performed for both cases, case 4 and case 5, although it was clear that the maximal temperature is higher than the measured temperature. The same velocity has been chosen since the rounded values, obtained from the heat input values given in Table 2, are the same. The calculated value of cooling time from 800°C to 500°C for the case 4 of cca 38 s is much higher than the measured value of 28 s. The same applies to the numerical result for the cooling time of case 5, the numerical value is 23 s while the measured value is 16 s.

Conclusion

The selected series of experimental results was divided into two groups. A criterion was the characteristic of the heat source or, more precisely, the characteristic of the electrode. An available input data was the heat input, and an available output data was the maximal value of temperature at only one point in the heat effected zone and the cooling time from 800°C to 500°C for that point. Numerous calculations have been executed in an attempt to set the parameters of the numerical heat source. The double ellipsoidal heat source is complex, the possibilities are numerous, but the question still stands – how to decide which the correct principle of selection of parameters is.

References

- [1] M. Berkovic, S. Maksimovic and A. Sedmak, "Analysis of Welded Joints by Applying the Finite Element Method," *Structural Integrity and Life*, 4 (2004), 2, pp. 75-83.
- [2] V. N. Lazic, A. S. Sedmak, M. M. Zivkovic, S. M. Aleksandrovic, R. D. Cukic, R. D. Jovicic and I. B. Ivanovic, "Determining Of Cooling Time ($t_{8/5}$) In Hard Facing Of Steels For Forging Dies," *Thermal science*, 14 (2010), 1, pp. 235-246.
- [3] S. Cvetkovski, L. P. Karjalainen, V. Kujanpaa and A. Ahmad, "Welding Heat Input Determination In TIG And Laser Welding of Ldx 2101 Steel by Implementing The Adams Equation For 2-D Heat Distribution," *Structural Integrity and Life*, 10 (2010), 2, pp. 103-109.
- [4] D. Kalaba, A. Sedmak, Z. Radakovic and M. Miloš, "Thermomechanical Modeling the Resistance Welding of Pbsb Alloy" *Thermal Science*, 14 (2010), 2, pp. 437-450.
- [5] W. Perret, C. Schwenk and M. Rethmeier, "Comparison of analytical and numerical welding temperature field calculation," *Computational Materials Science*, 47 (2010), 4, pp. 1005-1015.
- [6] J. Goldak, A. Chakravarti and M. Bibby, "A New Finite Element Model for Welding Heat Sources," *Metallurgical transactions B*, 15 (1984), 2, pp. 299-305.
- [7] M.C. Smith and A.C. Smith, "NeT bead-on-plate round robin: Comparison of transient thermal predictions and measurements," *International Journal of Pressure Vessels and Piping*, 86 (2009), 1, pp. 96-109.
- [8] A. Pahkamaa, L. Karlsson, J. Pavasson, M. Karlberg, M. Nasstrom and J. Goldak, "A Method To Improve Efficiency In Welding Simulations For Simulation Driven Design," in *ASME 2010 International Design Engineering Technical Conference & Computers and Information in Engineering Conference IDETC/CIE 2010*, Montreal, Quebec, Canada, 2010.
- [9] J. Goldak, M. Asadi and R. Garcia Alena, "Why power per unit length of weld does not characterize a weld" *Computational Materials Science*, 48 (2010),2, pp. 390-401.
- [10] Veljic, M. Perovic, A. Sedmak, M. Rakin, N. Bajić, B. Medjo, H. Dascau, Numerical Simulation of the Plunge Stage in Friction Stir Welding, *Structural Integrity and Life*, 11 (2011), 2, pp.131-134.
- [11] I. Atanasovska, D. Momčilović, M. Burzić, T. Vuherer, Coupled Nonlinear Problems in Finite Element Analysis – A Case Study, *Structural Integrity and Life*, 12 (2012), 3, pp.201-208.
- [12] V. N. Lazic, *Optimization of surface welding process from the point of view of tribological characteristics of surface layer and residual stress (in Serbian)*, Ph.D. Thesis, Faculty of Mechanical Engineering, University of Kragujevac, Serbia, 2000.
- [13] Code Aster, "Documentation version 11" [Online]. Available: www.code-aster.org.

Paper submitted: January 17, 2013

Paper revised: June 19, 2013

Paper accepted: October 24, 2013